AFRL-AFOSR-VA-TR-2022-0129

Chiral Interlayer Rotations for Atomically-Thin Layered Metamaterials

Park, Jiwoong
UNIVERSITY OF CHICAGO THE
5801 S ELLIS AVE
CHICAGO, IL,
US

04/04/2022
Final Technical Report

Air Force Research Laboratory
Air Force Office of Scientific Research
Arlington, Virginia 22203
Air Force Materiel Command

REPORT DOCUMENTATION PAGE

PLEASE DO NOT RETURN YOUR FORM TO THE ABOVE ORGANIZATION.

1. REPORT DATE	2. REPORT TYPE	3. DATES COVERED	
20220404	Final	START DATE 20160815	END DATE 20210814

4. TITLE AND SUBTITLE
Chiral Interlayer Rotations for Atomically-Thin Layered Metamaterials

5a. CONTRACT NUMBER	5b. GRANT NUMBER	5c. PROGRAM ELEMENT NUMBER
	FA9550-16-1-0347	61102F
5d. PROJECT NUMBER	**5e. TASK NUMBER**	**5f. WORK UNIT NUMBER**

6. AUTHOR(S)
Jiwoong Park

7. PERFORMING ORGANIZATION NAME(S) AND ADDRESS(ES)
UNIVERSITY OF CHICAGO THE
5801 S ELLIS AVE
CHICAGO, IL
US

8. PERFORMING ORGANIZATION REPORT NUMBER

9. SPONSORING/MONITORING AGENCY NAME(S) AND ADDRESS(ES)	10. SPONSOR/MONITOR'S ACRONYM(S)	11. SPONSOR/MONITOR'S REPORT NUMBER(S)
Air Force Office of Scientific Research 875 N. Randolph St. Room 3112 Arlington, VA 22203	AFRL/AFOSR RTB1	AFRL-AFOSR-VA-TR-2022-0129

12. DISTRIBUTION/AVAILABILITY STATEMENT
A Distribution Unlimited: PB Public Release

13. SUPPLEMENTARY NOTES

14. ABSTRACT
The interlayer rotation angle is an exciting new degree of freedom in 2D layered materials (2DLMs), and its precise control has recently produced metamaterials including van der Waals
moire crystals with many emergent phenomena that are not found in nature. As these 2DLM multilayers with non-zero interlayer rotations are not thermodynamically preferred in growth,
they must be made artificially layer-by-layer with single layer building blocks with a predetermined lattice orientation.

The main aim of this project is to develop atomically thin metamaterials based on 2DLMs with tunable physical properties by precisely programing the interlayer structures in their multilayer
stacks. There are significant materials issues that need to be addressed in order to produce multilayer stacks and 2DLM-based films that are contamination-free and fully controlled. This
final report describes the development and application of the new synthesis, fabrication, characterization techniques our group has developed for studying fundamental structural and
optical properties in 2D materials, including mono- and multi-layers of transition metal dichalcogenides (TMDs) and their molecular analogs, as funded by the AFOSR grant (FA9550-16-1-0347).

First, we have developed approaches to grow high quality monolayer TMDs with precisely controlled electronic properties. This includes the synthesis of coherent lateral WS2/WSe2 superlattices with defect free interfaces and MoS2 monolayers with substitutional Nb-dopants. Second, we have developed fabrication and stacking approaches that are optimized for TMD
films with pristine interfaces. This includes a new resist-free lithography method and “robotic 4D pixel assembly” that automatically stacks TMD based pixels with high throughput. Third,
we have discovered and tuned novel optical properties of TMD films and stacks. This includes the optically isotropic TMD films with 3D corrugation and atomically thin optical waveguides
that launch micrometer thick, collimated optical beams. Finally, we have developed an exciting new approach of generating wafer-scale molecule-based 2D films using solution interface
synthesis that could allow for the realization of the exciting science of 2DLMs with molecule-based quantum solids.

15. SUBJECT TERMS

16. SECURITY CLASSIFICATION OF:			17. LIMITATION OF ABSTRACT	18. NUMBER OF PAGES
a. REPORT U	b. ABSTRACT U	c. THIS PAGE U	UU	17
19a. NAME OF RESPONSIBLE PERSON JIWEI LU			19b. PHONE NUMBER *(Include area code)* 00000000	

FA9550-16-1-0347
Final Report

COVER SHEET

Title:
CHIRAL INTERLAYER ROTATIONS FOR ATOMICALLY THIN LAYERED METAMATERIALS

Date:
March 31, 2022

Reporting Period:
Aug 2016 – Jul 2021

Organizations
University of Chicago, Chicago, IL

Program Manager
Dr. Jiwei Lu and Dr. Ali Sayir

TECHNICAL POC
Name: **Jiwoong Park**
Street Address**: 929 E. 57th Street (GCIS E219)**
University of Chicago
Chicago, IL 60637

Telephone: (773) 834-3179
Email: jwpark@uchicago.edu

Executive Summary

The interlayer rotation angle is an exciting new degree of freedom in 2D layered materials (2DLMs), and its precise control has recently produced metamaterials including van der Waals moire crystals with many emergent phenomena that are not found in nature. As these 2DLM multilayers with non-zero interlayer rotations are not thermodynamically preferred in growth, they must be made artificially layer-by-layer with single layer building blocks with a predetermined lattice orientation.

The main aim of this project is to develop atomically thin metamaterials based on 2DLMs with tunable physical properties by precisely programing the interlayer structures in their multilayer stacks. There are significant materials issues that need to be addressed in order to produce multilayer stacks and 2DLM-based films that are contamination-free and fully controlled. This final report describes the development and application of the new synthesis, fabrication, characterization techniques our group has developed for studying fundamental structural and optical properties in 2D materials, including mono- and multi-layers of transition metal dichalcogenides (TMDs) and their molecular analogs, as funded by the AFOSR grant (FA9550-16-1-0347).

First, we have developed approaches to grow high quality monolayer TMDs with precisely controlled electronic properties. This includes the synthesis of coherent lateral WS_2/WSe_2 superlattices with defect free interfaces and MoS_2 monolayers with substitutional Nb-dopants. Second, we have developed fabrication and stacking approaches that are optimized for TMD films with pristine interfaces. This includes a new resist-free lithography method and “robotic 4D pixel assembly” that automatically stacks TMD based pixels with high throughput. Third, we have discovered and tuned novel optical properties of TMD films and stacks. This includes the optically isotropic TMD films with 3D corrugation and atomically thin optical waveguides that launch micrometer thick, collimated optical beams. Finally, we have developed an exciting new approach of generating wafer-scale molecule-based 2D films using solution interface synthesis that could allow for the realization of the exciting science of 2DLMs with molecule-based quantum solids.

TECHNICAL DESCRIPTION OF WORK

Overview. Below we provide technical descriptions of our main achievements during the grant period (2016-2021) organized along four main categories. They are: (I) ***Generation*** of highly engineered TMD monolayers; (II) ***Patterning*** and ***Stacking*** for TMD pixels; (III) TMD films as novel ***Optical Elements***; and (IV) synthesis of ***2D Molecular films***. We will also briefly describe additional collaborative research results at the end. Our research has resulted in:

- **12 publications** including 2 in *Science*, 1 in *Nature Nanotechnology* ,1 in *Nature Photonics*, and 1 currently under revision in *Nature*. The full list of publications is included at the end of this report.
- **Three patents** are filed (2 full US application and 1 provisional – all pending) by the University of Chicago based on this research.
- Four researchers who worked on this project have become faculty members at leading research universities. They are **Saien Xie** (Princeton, ECE, Jan 2022), **Andrew Mannix** (Stanford, MSE, July 2020), **Yu Zhong** (Cornell, MSE, July 2022), and **Myungjae Lee** (Seoul National University, MSE, March 2022).

A. Generation of highly engineered TMD monolayers

A1. Lateral TMD pn-junctions with large bandgap materials.[1] Lateral or vertical assembly of heterogeneous transition metal dichalcogenides (TMDs) is the key technology to realize TMD-based optoeletronic devices. In particular, seamless lateral TMD heterostructures can only be achieved during material growth step with the constituent elements individually and precisely controlled during the growth. This makes our metal-organic chemical vapor deposition (MOCVD) process an ideal approach. During this grant, we demonstrated lateral

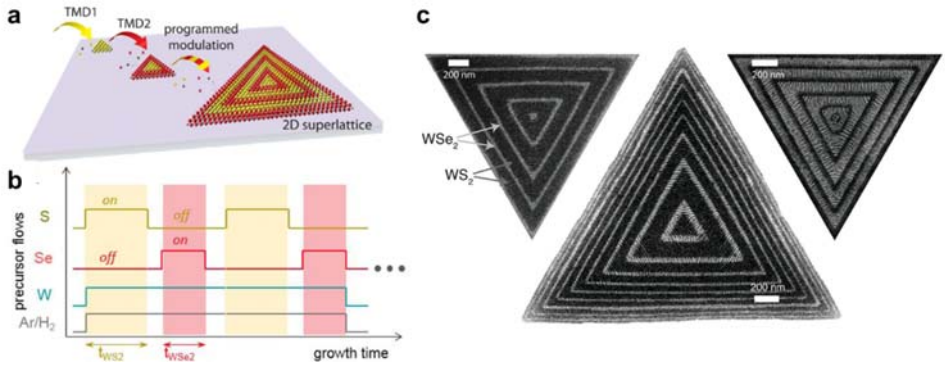

Figure 1 (a) Schematic of 2D superlattices based on monolayer TMDs. (b) Time sequence of the modulated superlattice growth where the growth time for a supercell {WS_2 and WSe_2} is {t_{WS2} and t_{WSe2}}. (c) SEM images of three monolayer WS_2/WSe_2 superlattices. Scale bars, 200 nm

heterostructure of monolayer WS_2/WSe_2 through programmed modulation of precursor injection during the growth (Figure 1a) At an optimized lateral growth conditions both for WS_2 and WSe_2, simple alternation of S and Se precursors (Figure 1b) resulted in concentric triangular shape heterostructure where dark and bright regions correspond to WS_2 and WSe_2, respectively. (Figure 1c) The width of each region can be finely tuned by adjusting chalcogen (S/Se) precursor injection time. Surprisingly, structural characterization (with TEM) revealed that our heterostructures have seamless epitaxial interface without dislocations, and this is also evidenced by the out-of-plane ripples generated by the difference in the lattice constants (~4%) of the two TMDs.

The dislocation-free heterointerfaces with precisely controlled nanoscale supercell dimensions are crucial for producing practical devices that are difficult to produce otherwise. To demonstrate this, we have fabricated and examined p-n junction devices based on our coherent WS_2 (intrinsic n-type) /WSe_2 (intrinsic p-type) superlattice heterostructures (Figure 2a). A representative p-n diode shows high forward-bias current (>10 μA) and low reverse-bias current (~10 pA), producing a high rectification ratio (>10^6). The high performance for our p-n diodes is consistent with the dislocation-free coherent heterointerfaces, as the coherent interfaces could minimize the scattering of

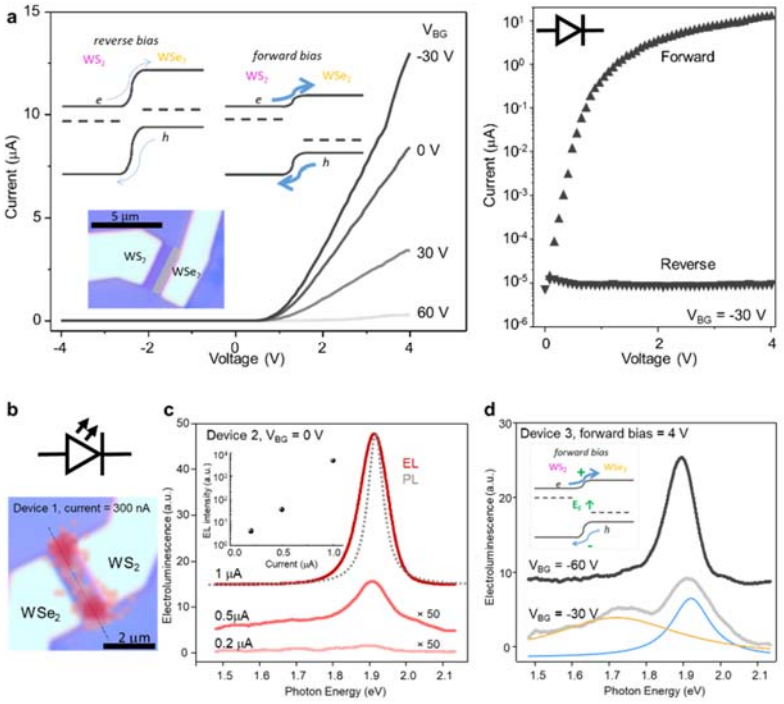

Figure 2 Electrical transport and electroluminescence of WSe_2/WS_2 p-n diodes. (a) Current-Voltage (I-V) curves for a WSe_2-WS_2 p-n diode under different V_{BG} showing a rectification ratio of 10^6. (b) EL intensity (red) map overlaid with optical micrograph of the p-n diode device, showing the EL centered at WS_2-WSe_2 heterointerface (marked with dashed line). (c) EL spectra (red) under current I = 0.2, 0.5, and 1 μA, respectively, together with PL spectrum (grey). Inset: EL intensity for corresponding current intensity, showing an exponential dependence. (d) EL spectra recorded under V_{BG} = -60 and -30 V, with fitted peaks (blue and orange) and the band diagram shown in inset.

carriers by dislocations, resulting in a higher electrical conductivity under forward bias. Furthermore, the defect-assisted hopping transport of charge carriers will be minimized, which accounts for a lower conductivity under reverse bias. We further observed strong electro-luminescence (EL) from the p-n diodes which function as LEDs. The EL is observed under the forward-bias condition, and its intensity dramatically increases with the injected current (I). For example, the EL from the device in Figure 2c increases by three orders of magnitude when the current increases only by a factor of 5 (inset, Figure 2c). The EL spectrum shows a peak similar to the PL peak from WS_2, which suggests that the light emission is likely to originate from the electron-hole recombination within WS_2. These observed features for EL and the back gate dependence (Figure 2d) matches very well with the expected band alignment (Figure 2d inset). The high current needed for EL and the efficient radiative recombination both require the absence of dislocations. Therefore, the observation of EL suggests that the coherent heterointerface is crucial for high-performance LEDs. We note that all our devices are directly fabricated on the SiO_2/Si growth substrate without any encapsulation and the EL measurements were performed under ambient conditions. This suggests that its performance (brightness and stability) may be further improved. Our study on WS_2/WSe_2 superlattice presents a viable route to produce high quality 2D TMD building blocks with spatially modulated bandstructures. This heterostructure formation is not limited to WS_2 and WSe_2 but can be extended to a wide range of TMD materials.

A2. Wafer-scale TMD synthesis with controlled doping.[2] We successfully developed a synthesis method for wafer-scale monolayer TMDs with controlled substitutional doping. Our approach is based on MOCVD growth technique through programmed modulation of precursor injection. It can be used for Nb, a hole-dopant, and Re, an electron-dopant, with precisely controlled doping levels. Figure 3a shows a schematic of the experimental setup for substitutional doping of MoS_2, where $NbCl_5$ (or Re_2CO_{10}) is introduced and precisely controlled in gaseous form to provide elemental Nb (or Re) during the growth of MoS_2. The presence of these substitutional dopants is confirmed by the scanning transmission electron microscopy (STEM) data shown in Figure 3b and 3c, each taken from Re-doped MoS_2 with different doping levels (2% vs 10%). Here, the bright spots correspond to Re atoms, which are found directly on the lattice sites of Mo without aggregation.

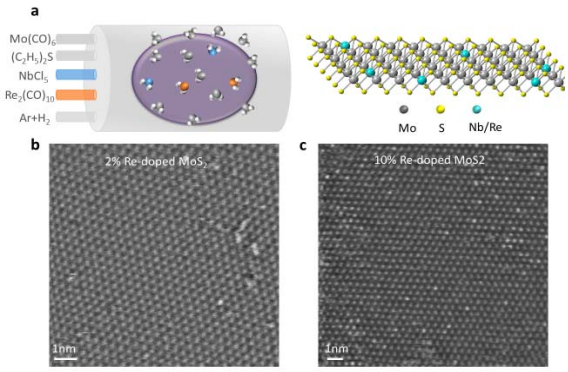

Figure 3. Monolayer MoS_2 with n-/p-type doping. (a) Schematic of the Re and Nb-doped MoS_2 synthesis. (b) and (c) are STEM images of 2% Re and 10% Re-doped MoS_2, respectively.

The doping is spatially homogeneous in large scale. Figure 4a shows an optical image of a Nb-doped MoS_2 device array that are fabricated over the entire area of 4 by 4 cm. The electrical resistance is uniform for these devices as shown by the map (right) of square resistance measured from a 5 by 5 device array. The Nb-doped MoS_2 shows *p*-type conduction; the gate transfer curve (Figure 4b) shows higher conductivity as the backgate voltage becomes more negative. The square resistance of the resulting *p*-type devices can be directly tuned by varying the Nb doping levels as shown in the histogram of device resistances (Figure 4c), where 100 devices are measured and plotted for each doping level.

In particular, the electrical conductivity of Nb doped MoS_2 under no electrostatic gating is reproducibly tuned over seven orders of magnitude by controlling the Nb concentration, displaying an exponential, instead of linear, dependence. Our study further indicates that the dopant carriers do not fully ionize in the 2D limit unlike in their 3D analogues, a conduction regime explained by the impurity band conduction. Moreover, we showed that the dopants are stable, enabling the doped films to be further processable as independent *p*-type building blocks that can be used as conductive electrodes.

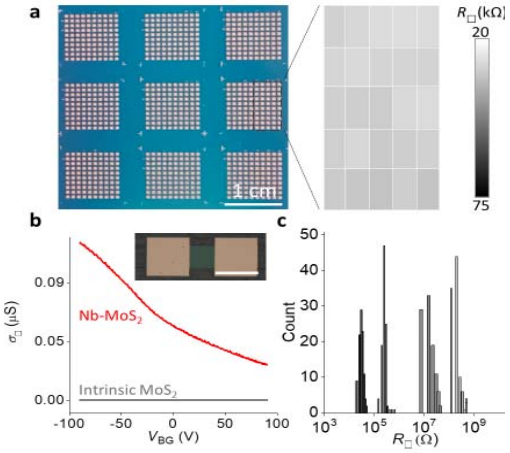

Figure 4. Wafer-scale doping for integrated circuits. (a) Optical micrograph of an array of Nb-doped MoS_2 devices (left) and square resistance map (right). (b) A gate transfer curve of a representative Nb-doped device. Inset: a false-colored optical image of our device. Scale bar 500 μm. (c) Electrical resistance histograms for 4 different doping levels (each from 100 devices).

B. Patterning and Stacking for TMD pixels

B1. Non-perturbative electrical measurements of atomically thin semiconductors.[3] It is well known that the electrical performance of semiconductor devices is determined by properties of semiconductor material and effects of processes it goes through during device fabrication. The main approach currently used for their electrical measurements, which involves lithography-based device fabrication, cannot provide accurate measurements as the act of measurement itself affects the measured outcome. To achieve controllable properties of TMD-based building blocks, we developed a non-perturbative method for electrical measurements as shown in Fig. 5a. It involves, (i) defining of MoS_2 channel areas using laser and, (ii) making actual electrical contacts to MoS_2 by transferring gold electrode/spacer bilayers onto the MoS_2 film using a polydimethylsiloxane (PDMS) stamp. They are used for conductivity ($\sigma_{\square}$) measurements (iii). Figure 5b shows an optical image of a completed electrode array. Figure 5c shows $\sigma_{\square}$ - V_{BG} curves (solid lines) measured non-perturbatively from MoS_2 channels, all of which show similar behaviors. In comparison, similar MoS_2 films with channels and electrodes defined using photolithography (dotted line) and further upon hafnium oxide deposition (dashed line) show different (and higher) values of $\sigma_{\square}$. Figure 5d shows a similar comparison using monolayer WSe_2. With non-perturbative measurements, the WSe_2 channels exhibit higher $\sigma_{\square}$ at negative V_{BG} compared to channels when measured via

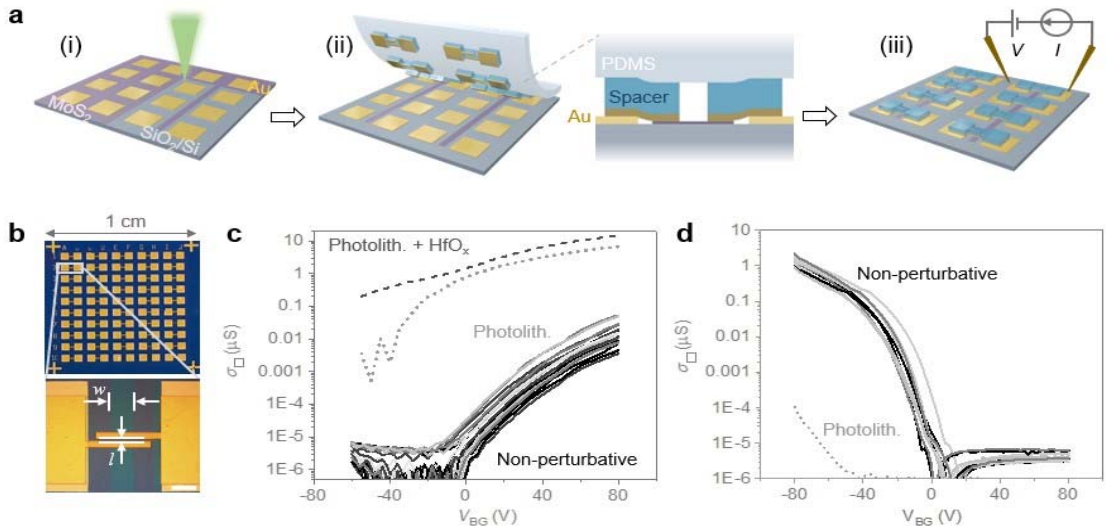

Figure 5 (a) Schematic of non-perturbative measurement method. (b) Photograph of fabricated MoS_2 transistor array over a square cm area. Zoomed in is an optical image of a pair of transferred electrodes, scale bar is 100 μm. (c) and (d) Sheet conductivity vs back gate voltage for MoS_2 and WSe_2 channels respectively. Solid lines: non-perturbative measurement; Dotted lines: photolithography-based measurements.

photolithography-based approach (dotted line). Our data suggests that MoS_2 channels exhibit lightly doped, *n*-type conductivities while the WSe_2 channels show a *p*-type behavior. In our experiment, the particular photolithography process leads to a further *n*-type doping of the TMD channels, increasing $\sigma_{\square}$ of MoS_2, which is *n*-type as grown, and decreasing $\sigma_{\square}$ of WSe_2, which is *p*-type.

In order to understand the observed *n*-doping during photolithography, we studied the change in $\sigma_{\square}$ of MoS_2 channels during conventional lithography steps using non-perturbative measurements. We use e-beam lithography (EBL) as an example process. Figure 6a shows schematic of MoS_2 channels during processes that involve PMMA coating (2), e-beam exposure (3), development (4) and exposure to acetone lift-off solvent after PMMA coating (5). The $\sigma_{\square}$ of non-exposed MoS_2 channel (1) is taken as a reference. Figure 6b shows $\sigma_{\square}$ - V_{BG} curves measured from channels after different processes. We observe that the transfer curves shift progressively from (1) to (4). However, the maximum $\sigma_{\square}$ increase is observed when PMMA is removed in acetone. Upon doing a similar study for conventional *photo*lithography process (Fig. 6c), we again observe major increment in conductivity for processes involving developers and acetone solvent. This is different from a widely held belief that resist coating changes the electrical properties of TMD materials the most. This technique offers a generalizable tool for precisely measuring and controlling electrical properties of 2DLMs as grown and after each process step.

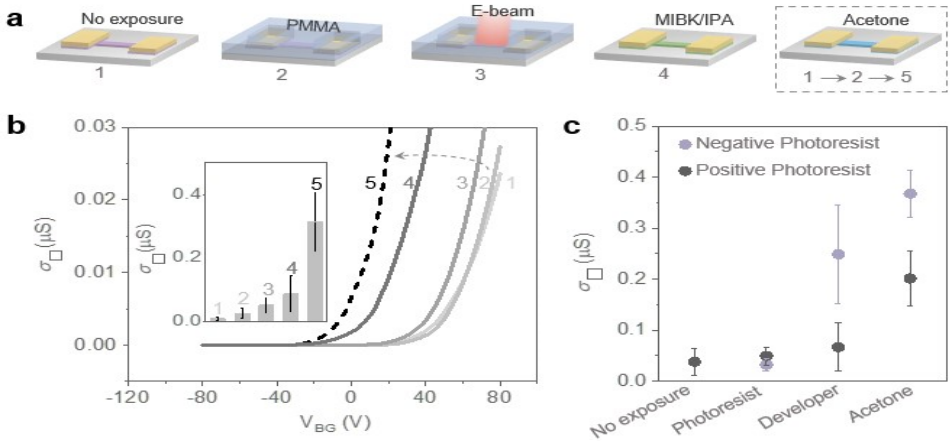

Figure 6 (a) Schematic of MoS_2 channels at various processing steps involving different fabrication elements during EBL. (b) Representative transfer curves of non-exposed MoS_2 and ones obtained at numerically designated process steps in Fig. 6a of EBL. Inset: Columns correspond to mean on-state conductivity from 15 devices at each step. (c) Mean on-state conductivity obtained from MoS_2 channels at process steps during photolithography.

B2. Automated Vacuum Fabrication of van der Waals Heterostructures.[4] The construction of atomically-resolved heterostructures provides the ultimate degree of precision in materials engineering. The assembly of atomically thin materials restacked into van der Waals (vdW) heterostructures provides an ideal platform to realize this vision. Although previous approaches were limited primarily to small mechanically-exfoliated flakes, we recently demonstrated wafer-scale construction of high-quality vdW heterostructures using synthesized monolayer materials discussed in **Section A**. Based on this concept, we envision the arbitrary patterning of wafer-scale materials into functional sub-units ("pixels") which can be assembled on-demand into a wide variety of vdW superlattices or device heterostructures (Figure 7a). These pixel units have been patterned by various polymer-free lithography techniques developed during this grant period (Figure 7b). We can access the pixels individually (or in multiples, as needed) using polymeric micromanipulators, which provides programmed adhesion with thermal release stimulus (Figure 7c). These manipulators, and the desired substrates, are mounted in a 4-axis micromanipulation stage (Figure 7d), which is contained under vacuum conditions to reduce adventitious contamination between the stacked layers (thereby also enabling fabrication with air-sensitive materials).

Using this system, our micromanipulator stamps are capable of picking up and depositing a single monolayer (e.g., MoS_2, WS_2, etc. Figure 8a), or more complex multilayered structures

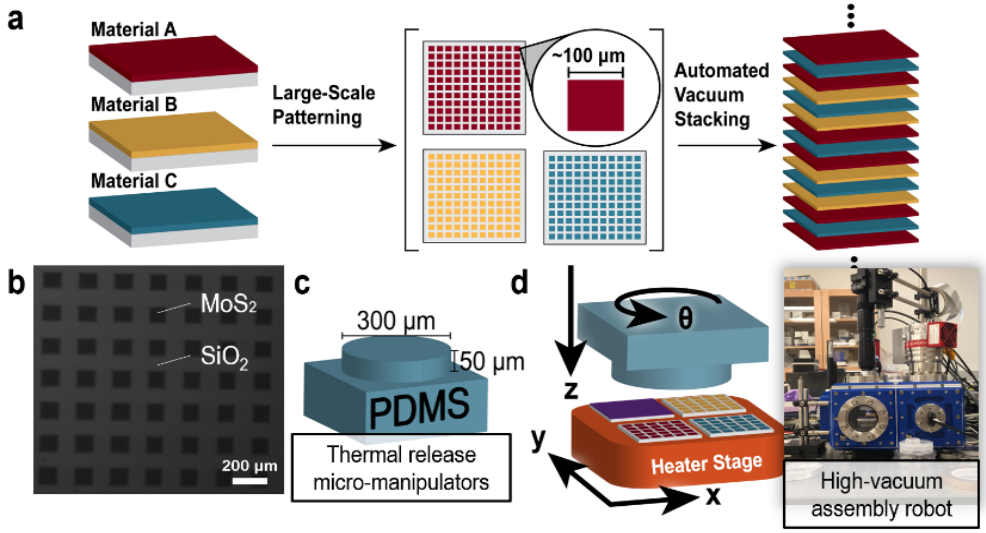

Figure 7: (a) Schematic of automated heterostructure fabrication scheme. (b) Optical micrograph of patterned MoS_2 "pixels." (c) Schematic of polymer micromanipulator. (d) Schematic of robotic manipulation degrees of freedom. (inset: photo of constructed robotic stacking setup).

(Figure 8b). This approach can be used to generate superlattices with atomic resolution (Figure 8c) using a variety of 2D material building blocks. These capabilities establish functional parity with the state-of-the-art exfoliation-based vdW heterostructure fabrication techniques but provide significant advantages in terms of scale and throughput (e.g., factor of ~10^2 larger area and ~10^2 faster). At present, we have constructed heterostructures up to 30 layers, and have encountered no fundamental limitation to heterostructure thickness.

Our methodology promises significant enhancements in the fundamental capabilities of 2D-based vdW heterostructure fabrication. The recent demonstration of strongly-correlated electronic states and superconductivity in "magic angle" rotationally twisted bilayers of graphene promises unprecedented opportunities for electronic structure engineering based on the tunable interlayer interactions in vdW heterostructures. However, the results to date have been constrained by the microscopic sample size of exfoliated flakes, limiting the number of aligned layers to ~2-3. In contrast, our automated vdW heterostructure fabrication faces no such limits for rotationally aligned stacking (demonstrated in Figure 8d and 8e). If combined with ongoing efforts towards epitaxially aligned growth, we can explore the properties of an essentially unlimited number of twisted layers, culminating in the synthesis of a wide range of rotationally structured quantum solids.

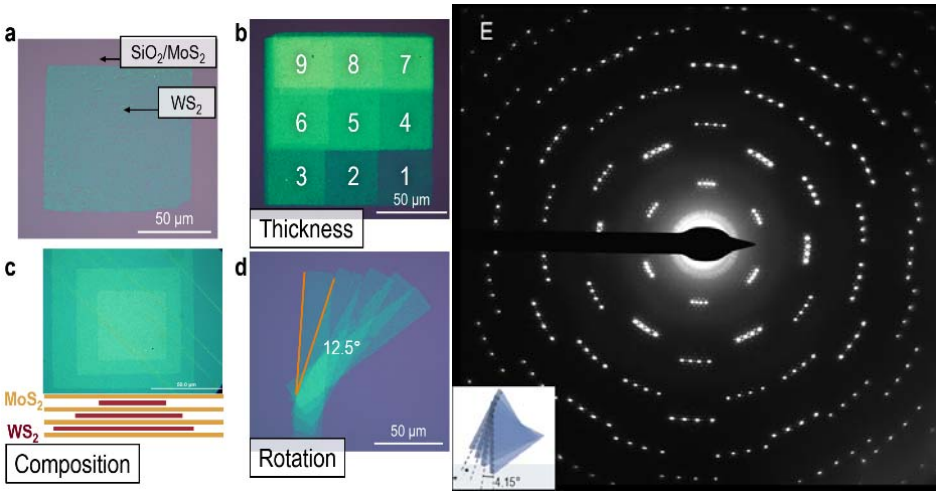

Figure 8 Optical micrographs of: (a) transferred monolayer WS_2 pixel. (b) WS_2 multiple thickness test structure (layer number is overlaid). (c) Composition superlattice (inset: diagram of atom-resolved composition). (d) WS_2 Interlayer rotation test structure. (e) TEM diffraction image of a 4-layer WS2 stacked with 4° interlayer angles.

C. TMD films as novel Optical Elements

C1. Nanodome-designed monolayer TMD films for isotropic angular response.[5] Atomically thin 2DLMs, thanks to their variety of intriguing properties and their high tunability, enable the active manipulation of light flow in the ultimate limit of thinness. However, existing research on 2D material-based flat optics still remains in a nascent period of development. One bottleneck is the poor light absorption for light introduced to a 2D film with a high angle, originating from an intrinsic property of a 2DLM—optical anisotropy. During this grant, we developed an approach to present a general solution to this challenge: 3D reorientation of anisotropic 2D crystals.

The main idea is to use 3D nanotopography to control the anisotropy of atomically thin materials at three different length scales, here realized using conformal growth of monolayer TMDs on nanodome structures. Macroscopically, the films are optically flat, just like an ordinary thin film with wafer-scale homogeneity, showing our synthesis is fully scalable and generally applicable to different TMD materials (Figure 9a). On the nanoscale, the locally flat surface of 3D geometry is conformally covered with an unstrained monolayer TMD, which maintains its intrinsic properties (Figure 9b). On the intermediate (~100 nm) length scale, however, 3D structuring allows us to control the orientations of the anisotropic crystals and manipulate their light-matter interactions in the near-field regime (Figure 9c). For example,

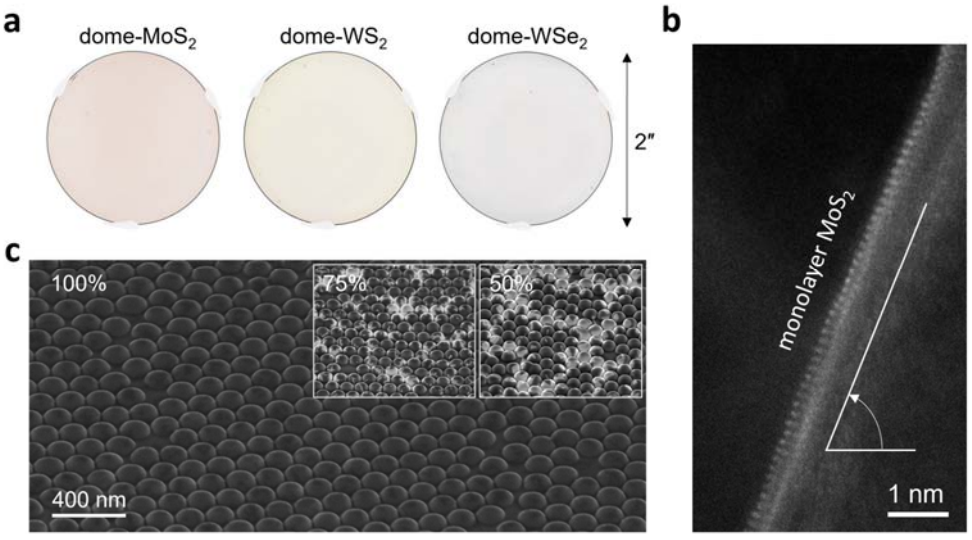

Figure 9 *Nanotextured monolayer TMD films.* (a) Versatile monolayer TMD films with 3D nanodome designed topography. (b) SEM images of dome textured monolayer MoS_2 with different surface coverage. (c) Atomic arrangement of monolayer MoS_2 imaged by HAADF-STEM.

nanostructured TMD films provide a one-order-of-magnitude enhancement in the out-of-plane susceptibility, which balances the in-plane response.

As a result, we observe wide-angle optical responses, polarization isotropy in absorption, and more uniform emission in photoluminescence. Figure 10a shows that, despite the anisotropic nature of monolayer MoS_2, our dome-MoS_2 displays the polarization isotropy, which further enhances the total light absorption at large incidence angles. This confirms that the 3D restructuring of anisotropy is an ideal approach to control and enhance the angular performance of 2D materials in a predictable manner, producing atomically thin, optically isotropic films, while at the same time maintaining the intrinsic material properties. Our approach for isotropy is not limited to light absorption, but also applicable to light emission. While light emission from flat surfaces is directional (from the surface normal), dome-MoS_2 provides a more isotropic angular profile. The difference between two profiles, displayed in Figure 10b, ($\Omega_{dome}-\Omega_{flat}$) shows that the photoluminescence (PL) uniformity is significantly improved at higher angles (bright yellow ring). The angular plot of the differential change $(\Omega_{dome}-\Omega_{flat})/\Omega_{flat}$ monotonically increases, compensating for the deficiency of light emission from the flat surface at grazing angle (Figure 10c).

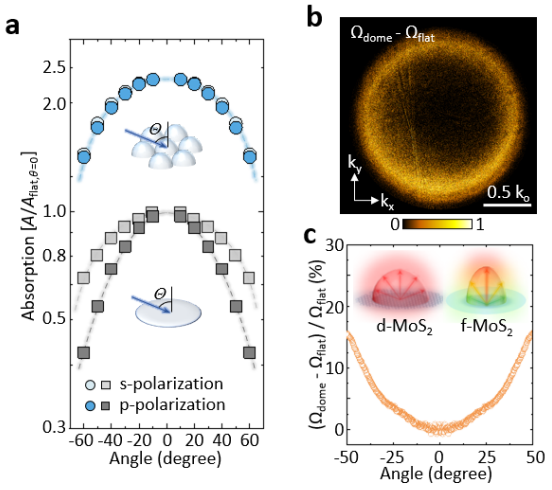

Figure 10 *Wide-angle and angular isotropy in optical properties.* (a) Angular absorption with s- and p-polarized light in dome- and flat-MoS_2. (b) Angular difference of emission profiles between dome- and flat-MoS_2 by PL. (c) Differential PL enhancement as a function of emission angle.

C2. Atomically thin δ-waveguides for 2D photonics.[6] We showed that atomically thin TMD film alone (that is, without any photonic structures) guides light waves over millimeter length scale, which is long enough to realize photonic circuitry. We used a monolayer MoS_2 film directly grown on fused silica substrate that offers wafer-scale uniformity of atomically thin guiding geometry, which is activated in carefully designed liquid environment to provide symmetric dielectric environment across the substrate and the liquid (Figure 11). We investigated our system by edge-on incidence where probing photons are incident on the edge of the sample having ray trajectory parallel to the film surface and visualized optical fields on

the film through dark field microscopy where elastically scattered light is collected in film-plane-imaging geometry.

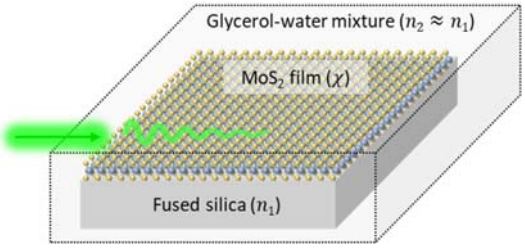

Figure 11 Schematic of atomically thin waveguide and edge-on incidence.

Our approach enables the guiding of electromagnetic wave over a wide range of photon energies including visible and near-infrared wavelengths (500 nm – 900 nm). The guided wave propagates in millimeter length-scale over the entire spectral range (Figure 12). The propagation length even reaches to centimeter scale at near-infrared wavelengths. We showed that the monolayer film offers the best propagation length over multi-layered films *and* that such a trend can be accurately explained by the strong exitonic interaction between the guided waves and the MoS_2 films. Such observation suggests that our system hosts a strong light-matter interaction amplified by the guiding geometry, making the interaction to propagate over a long distance.

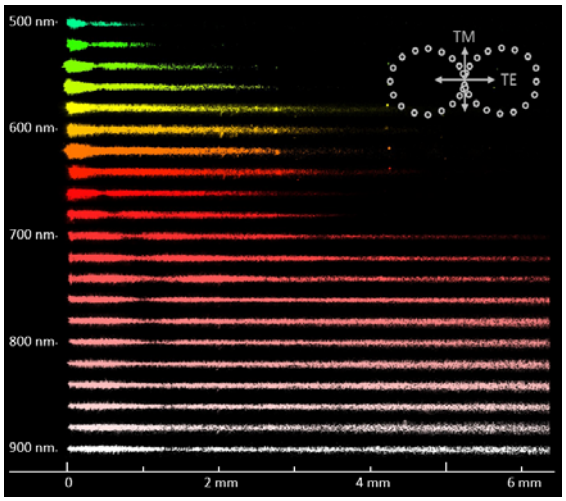

Figure 12 Visualization of guided wave as a function of wavelength

Furthermore, we demonstrated that such light guiding can be manipulated for photonics applications. The wavefront of propagation wave is controllable by shaping the excitation beam, presenting either converging or diverging profiles (Figure 13a). In addition to the wavefront shaping, we also showed that atomically thin optical geometries can be used to split and steer the guided wave within the waveguides (Figure 13b). Furthermore, by using an external stimuli field, we demonstrated the feasibility of actively switching wave propagation from nonlinear interaction between the pump and the probe beam.

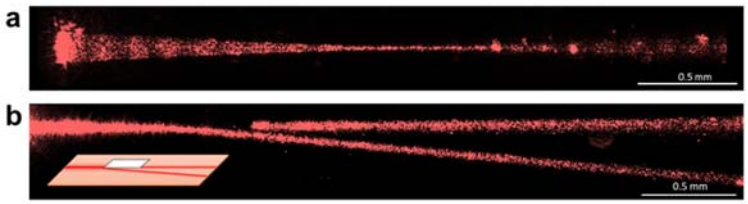

Figure 13 *Manipulation of guided waves.* (a) Wavefront modulation through incident beam shaping. (b) Beam splitting by atomically thin optical geometry.

D. Synthesis of 2D Molecular films

Wafer-Scale Monolayer Two-Dimensional Polymers.[7] Finally, we developed a modular approach to synthesize monolayer 2D polymers (2DPs) with wafer-scale homogeneity, which provides molecule-based 2D building blocks for vdW assembly for the first time. 2DPs are one-molecule-thick, freestanding films composed of molecules linked via covalent or coordination bonds in a periodic structure. Taking 2DPs as building blocks for designer thin films, we combine layer-by-layer assembly and molecular-level design, in a single materials platform. Several accomplishments have been made in this project, including (1) wafer-scale synthesis of various monolayer 2DPs, (2) development of general synthesis method for 2DPs growth, (3) patterning and integration of 2DPs lateral junctions, (4) and assembly of 2DP/MoS_2 vertical heterostructures.

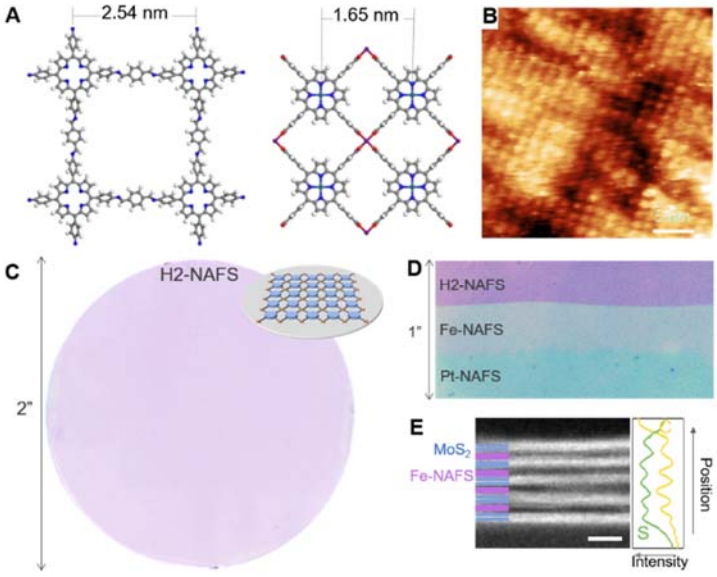

Figure 14 (a) Crystal structure of representative 2DPs: COF-366 (Left) and Pt-NAFS (Right). (b) STM image of Pt-NAFS. (c) False color image of 2-inch monolayer H2-NAFS. (d) False color image of NAFS lateral junctions. (e) Cross-sectional ADF STEM image (Left) and EELS profile (Right) of a MoS_2/Fe-NAFS superlattice film. Scale bar: 5 nm.

First, all the 2DPs display wafer-scale uniformity. Several 2DPs are synthesized by cross-linking various monolayer metallated porphyrins via coordination bonds (NAFS) or covalent bonds (COF-366) (Figure 14a). The crystallinity of the 2DPs are confirmed by XRD and visualized by scanning tunneling microscope (STM) (Figure 14b). Vertically, all the films are about 1 nm thick, consistent with the height of a single porphyrin molecule. Laterally, the 2DP films are continuous and uniform on a wafer scale (Figure 14c). Moreover, the as-synthesized 2DPs are freestanding and can be transferred onto various substrates.

Second, a modular synthetic method, called laminar assembly polymerization (LAP), has been developed to synthesize 2DPs. In this method, we harness the power of interfacial molecular

self-assembly and unidirectional laminar mass transport to rigorously control film thickness on a molecular level and film integrity over the size of a few inches. LAP is a scalable, low-cost, and general method to produce high-quality 2DP building blocks.

Third, the 2DP films can be patterned and assembled in a variety of ways. For example, utilizing the unique unidirectional transport, different kinds of 2DPs stitch in parallel to form lateral heterojunctions (Figure 14d). Besides, the 2DPs can be directly patterned on water surface and subsequently assembled into vertical heterostructures. The versatile process and integration capabilities offer tremendous opportunities to fabricate complicated 3D structures from 2DPs building blocks.

Finally, the 2DPs can be layer-by-layer assembled into vertical heterostructures with other 2DLMs such as MoS_2 with sub-nanometer precision (Fig. 14e). The structure was programmed by varying the composition of each layer, stacking sequence and the total number of layers. The hybrid van der Waals heterostructure charts a new pathway to create chemically and structurally versatile designer materials.

E. Additional Research Outcomes from Collaborative Efforts

In addition, our work in the past has led to a number of successful collaborations with published results. We presented comprehensive analysis on circular dichroism from interlayer rotation, by addressing effects of interlayer slip in addition to the rotation angle, which provides a complete model for manipulating the polarization state of light with geometric degrees of freedom in material processing.[8] We found that single exciton dynamics, not bi-excitonic excited-states, prevail in MoS_2 even at strong fluence near sub-Mott limit, which indicates that optoelectronic responses of 2D semiconductors is dominated by single-exciton features at practical illumination conditions.[9] On the other hand, at wavelengths far from exciton resonances where 2D semiconductor becomes transparent, we showed that electro-refractive response overwhelms excitonic absorption, which is distinct from common materials for silicon photonics so that enables novel photonic functions such as efficient phase modulator.[10] Lastly, we demonstrated that such atomically-thin layered materials can be self-folded into 3D reconfigurable optoelectronic circuitry by integrating it with thin polymer films, allowing us to explore geometric opportunities in 3D functional devices.[11] We have also developed a

theoretical method that predicts the local curvature of atomically thin membrane at nanometer length-scale, achievable with spontaneous alloy formation conforming onto predesigned 3D substrate at growth stage, which will allow us to geometrically program mechanical, optical, and electric properties of two-dimensional (2D) materials.[12]

F. Published Papers

(1) Xie, S.; Tu, L.; Han, Y.; Huang, L.; Kang, K.; Lao, K. U.; Poddar, P.; Park, C.; Muller, D. A.; DiStasio, R. A.; Park, J. Coherent, Atomically Thin Transition-Metal Dichalcogenide Superlattices with Engineered Strain. ***Science***. **2018**, *359*, 1131–1136.

(2) Gao, H.; Suh, J.; Cao, M. C.; Joe, A. Y.; Mujid, F.; Lee, K.-H.; Xie, S.; Poddar, P.; Lee, J.-U.; Kang, K.; Kim, P.; Muller, D. A.; Park, J. Tuning Electrical Conductance of MoS_2 Monolayers through Substitutional Doping. ***Nano Lett.*** **2020**, *20*, 4095–4101.

(3) Poddar, P. K.; Zhong, Y.; Mannix, A. J.; Mujid, F.; Yu, J.; Liang, C.; Kang, J.-H.; Lee, M.; Xie, S.; Park, J. Resist-Free Lithography for Monolayer Transition Metal Dichalcogenides. ***Nano Lett.*** **2022**, *22*, 726–732.

(4) Mannix, A. J.; Ye, A.; Sung, S. H.; Ray, A.; Mujid, F.; Park, C.; Lee, M.; Kang, J.; Shreiner, R.; High, A. A.; Muller, D. A.; Hovden, R.; Park, J. Robotic Four-Dimensional Pixel Assembly of van der Waals Solids. ***Nat. Nanotechnol.*** **2022**, DOI: 10.1038/s41565-021-01061-5.

(5) Lee, M.; Kang, J. H.; Mujid, F.; Suh, J.; Ray, A.; Park, C.; Muller, D. A.; Park, J. Atomically Thin, Optically Isotropic Films with 3D Nanotopography. ***Nano Lett.*** **2021**, *21*, 7291–7297.

(6) Lee, M.; Yu, J.; Mujid, F.; Ye, A.; Park, J. δ-Waveguides for Two-Dimensional Photonics. ***Nature.*** Under revision.

(7) Zhong, Y.; Cheng, B.; Park, C.; Ray, A.; Brown, S.; Mujid, F.; Lee, J.-U.; Zhou, H.; Suh, J.; Lee, K.-H.; Mannix, A. J.; Kang, K.; Sibener, S. J.; Muller, D. A.; Park, J. Wafer-Scale Synthesis of Monolayer Two-Dimensional Porphyrin Polymers for Hybrid Superlattices. ***Science.*** **2019**, *366*, 1379–1384.

(8) Addison, Z.; Park, J.; Mele, E. J. Twist, Slip, and Circular Dichroism in Bilayer Graphene. ***Phys. Rev. B*** **2019**, *100*, 125418.

(9) Wood, R. E.; Lloyd, L. T.; Mujid, F.; Wang, L.; Allodi, M. A.; Gao, H.; Mazuski, R.; Ting, P.-C.; Xie, S.; Park, J.; Engel, G. S. Evidence for the Dominance of Carrier-Induced Band Gap Renormalization over Biexciton Formation in Cryogenic Ultrafast Experiments on MoS_2 Monolayers. ***J. Phys. Chem. Lett.*** **2020**, *11*, 2658–2666.

(10) Datta, I.; Chae, S. H.; Bhatt, G. R.; Tadayon, M. A.; Li, B.; Yu, Y.; Park, C.; Park, J.; Cao, L.; Basov, D. N.; Hone, J.; Lipson, M. Low-Loss Composite Photonic Platform Based on 2D Semiconductor Monolayers. ***Nat. Photonics*** **2020**, *14*, 256–262.

(11) Xu, W.; Li, T.; Qin, Z.; Huang, Q.; Gao, H.; Kang, K.; Park, J.; Buehler, M. J.; Khurgin, J. B.; Gracias, D. H. Reversible MoS_2 Origami with Spatially Resolved and Reconfigurable Photosensitivity. ***Nano Lett.*** **2019**, *19*, 7941–7949.

(12) Berry, J.; Ristić, S.; Zhou, S.; Park, J.; Srolovitz, D. J. The MoSeS Dynamic Omnigami Paradigm for Smart Shape and Composition Programmable 2D Materials. ***Nat. Commun.*** **2019**, *10*, 5210.

G. Filed Patents

1. "Superlattice structure including two-dimensional material and device including the superlattice structure", US Patent Application, 16/428,006 (5/31/2019)
2. "Large Lateral Scale Two-Dimensional Materials and Other Thin Films, and Associated Systems and Methods", US Patent Application, PCT/US20/54378 (10/6/2020)
3. "Multi-Layer Stacks of 2D Materials and/or Other Layers and Related Systems and Methods", US Provisional Patent 63/284,541 (11/30/2021)